Roberts, J. W. (1976) in *RNA Polymerase* (Losick, R., & Chamberlin, M., Eds.) pp 247–271, Cold Spring Harbor Laboratory, Cold Spring Harbor, NY.
Rosenberg, A. H., Simon, M. N., Studier, F. W., & Roberts, R. J. (1979) *J. Mol. Biol. 135*, 907–915.
Sakai, T. T., & Cohen, S. S. (1976) *Prog. Nucleic Acid Res. Mol. Biol. 17*, 15–42.
Stahl, S. J., & Chamberlin, M. J. (1977) *J. Mol. Biol. 112*, 577–601.
Studier, F. W., Rosenberg, A. H., Simon, M. N., & Dunn, J. J. (1979) *J. Mol. Biol. 135*, 917–937.
Thomas, C. A., Jr., & Abelson, J. (1966) in *Procedures in Nucleic Acid Research* (Cantoni, G. L., & Davies, D. R., Eds.) pp 553–561, Harper and Row, New York.

Catalytic Mechanism of Phenylalanyl-tRNA Synthetase of *Escherichia coli* K10. Different Properties of Native and Photochemically Cross-Linked $tRNA^{Phe}$ Can Be Explained in the Light of tRNA Conformer Equilibria†

Eggehard Holler,* Mireille Baltzinger, and Alain Favre‡

ABSTRACT: Kinetic and equilibrium constants of phenylalanylation, AMP-dependent deacylation, and AMP-independent deacylation by phenylalanyl-tRNA synthetase of *Escherichia coli* K10 have been measured for $tRNA^{Phe}$ that was cross-linked by UV irradiation between uridine in position 8 and cytidine in position 13. The association of the aminoacylated tRNA with enzyme was investigated by stopped-flow techniques. The results are compared with those for native tRNA and Phe-tRNA. (1) Formation of the enzyme·substrate complexes follows dissociation constants and Michaelis–Menten complexes with 25-fold higher values for cross-linked in comparison to native tRNA. (2) Catalytic rate constants are the same for phenylalanylation of native and cross-linked $tRNA^{Phe}$. (3) Michaelis–Menten constants for AMP-dependent and -independent deacylation of Phe-tRNA have similar values for native and cross-linked $tRNA^{Phe}$. (4) The catalytic rate constant of AMP-dependent deacylation is 10^3-fold reduced in comparison to that of native Phe-tRNA, while that of AMP-independent deacylation is twice the value for native Phe-tRNA. (5) The kinetics of enzyme·Phe-tRNA complex formation are described by the same minimal reaction scheme as for native Phe-tRNA, a rapid binding equilibrium at the tRNA-specific binding site of the enzyme and a rate-determining binding at the phenylalanine-specific binding site of the enzyme [Holler, E. (1980) *Biochemistry 19*, 1397–1402]. The complex at the tRNA-specific site has a dissociation constant of 0.35 μM. This is similar to the K_m values for deacylation. Rate constants for dissociation of native and cross-linked Phe-tRNA from the phenylalanine-specific binding site have identical values. The same values have been found for the catalytic rate constants of phenylalanylation. The association of native Phe-tRNA to the Phe-specific binding site follows a rate constant that has a 25-fold higher value than that for cross-linked Phe-tRNA. Whereas for native Phe-tRNA the rate constants are the same for the association at the Phe-specific site and for the AMP-dependent deacylation, that of the association of cross-linked Phe-tRNA is 46-fold higher than the value of the rate constant for AMP-dependent deacylation. All the differences between native and cross-linked $tRNA^{Phe}$ are accounted for by a unifying model which assumes cross-link and phenylalanylation dependent conformer equilibria and which assumes the rate-limiting steps of phenylalanylation and AMP-dependent deacylation to be a conformational change during dissociation–association of Phe-tRNA at the phenylalanine-specific binding site of the enzyme.

The present work was initiated for two reasons. (1) Near-UV-induced growth delay of *Escherichia coli* has been discovered to be coupled to an intramolecular 8–13 cross-linking of tRNAs (Thomas & Favre, 1975; Ramabhadran & Jagger, 1976). Mutants have been grown which no longer exhibit the growth delay and which are deficient in 4-thiouridine, the chromophore responsible for cross-linking (Thomas & Favre, 1977). $tRNA^{Phe}$ has been found to play a key role. Upon irradiation of crude in vitro systems, initial rates of phenylalanylation were decreased to 5% of that of aminoacylation of other tRNAs by using conventional assay conditions (Carrê et al., 1974). We present here kinetic parameters of phenylalanylation and AMP-dependent deacylation for cross-linked $tRNA^{Phe}$ in comparison to that of native $tRNA^{Phe}$. The results are self-explanatory and support previous conclusions (Thomas & Favre, 1977).

(2) The reaction of cross-linking has been found to be inhibited by formation of a complex between $tRNA^{Phe}$ and phenylalanyl-tRNA synthetase of *E. coli* (Favre et al., 1979). Complex formation has been shown to favor a rearrangement of $tRNA^{Phe}$ that decreases the probability of occurrence of a transition state necessary for 8–13 link formation. Reciprocally, the number of conformations of $tRNA^{Phe}$ is expected to be decreased after cross-linking. The present work examines the effect of cross-linking on various steps of the catalytic reactions of phenylalanyl-tRNA synthetase in comparison to that of native $tRNA^{Phe}$. The results are interpreted by a unifying concept, which allows for conformer equilibria of

† From the Institut für Biophysik und Physikalische Biochemie, der Universität Regensburg, D-8400 Regensburg, Federal Republic of Germany. *Received July 10, 1980.* This work was supported by a NATO grant to E.H. and A.F. M.B. received an EMBO postdoctoral fellowship.
‡ Present address: Institut de Recherches en Biologie Moléculaire, Paris, 75005 France.

0006-2960/81/0420-1139$01.25/0

tRNA. The distribution of $tRNA^{Phe}$ into conformers is found to depend on cross-linking and phenylalanylation.

Materials and Methods

Phenylalanyl-tRNA synthetase (EC 6.1.1.20) has a specific activity of 53 000 nmol mg^{-1} h^{-1} (Hanke et al., 1974) and contained 2 active sites/molecule of enzyme (Bartmann et al., 1975a). L-[^{14}C]Phenylalanine (~500 μCi/μmol) was obtained from Radiochemical Centre (Amersham). Inorganic pyrophosphatase (EC 3.6.1.1), $tRNA^{Phe}$ (1300 pmol/A_{260} units phenylalanine acceptance), and ATP were purchased from Boehringer/Mannheim, 2-(*p*-toluidinyl)naphthalene-6-sulfonate and cetyltrimethylammonium bromide from Serva/Heidelberg, and all other reagents of highest possible grade from Merck/Darmstadt.

Nitrous acid treated $tRNA^{Phe}$ and DL-β-phenyllactyl-$tRNA^{Phe}_{HNO_2}$ were prepared exactly as described (Güntner & Holler, 1979). $tRNA^{Phe}_{h\nu}$[1] was obtained by UV irradiation according to Favre & Yaniv (1971). The yield of cross-linking was better than 99%, as judged by the sodium borohydride method (Favre & Yaniv, 1971).

Phenylalanylation of tRNA was carried out by the method of Kosakowski & Böck (1970). For initial velocity measurements, the reaction mixture (250 μL) was incubated for 15 s at 25 °C. In control measurements, it was verified that true initial rates were followed. The reaction mixture contained 0.1 M Tris-HCl buffer (pH 7.5), 10 mM KCl, 10 mM $MgCl_2$, 2 mM ATP, 2 mM reduced glutathione, 0.2 mM [^{14}C]Phe (10 μCi/μmol), 33 nM enzyme, and varying amounts of $tRNA^{Phe}_{h\nu}$. In the tRNA-charging assay, the reaction mixture contained fixed concentration of $tRNA^{Phe}_{h\nu}$, varying concentrations of enzyme, 50 μg/mL inorganic pyrophosphatase, and [^{14}C]Phe in a more than 5-fold excess over the amount of tRNA to be acylated besides the other reagents of the aminoacylation assay. The charging was terminated by addition of the 250-μL reaction mixture to 50 μL of unfractionated carrier tRNA (100 A_{260} units/mL in 0.5 M sodium acetate, pH 5) and immediate precipitation with 2 mL of 10% trichloroacetic acid.

Phenylalanyl-tRNA synthetase catalyzed hydrolysis of [^{14}C]Phe-$tRNA^{Phe}_{h\nu}$ (20 μCi/μmol) was followed by the method of Yarus (1972), employing precipitation of tRNA with cetyltrimethylammonium bromide at a final concentration of 0.5 mg/mL. The reaction was stopped by the addition of a tRNA carrier solution (final concentration of 6 A_{260}/mL in 0.1 M sodium acetate buffer, pH 5). The precipitate was removed by centrifugation at 5000*g*. Aliquots of the supernatant were dissolved in 5–10 mL of a hydrophilic scintillation cocktail, and radioactivity was counted in a Nuclear Chicago Isocap 300.

Steady-state deacylation of Phe-tRNA as catalyzed by phenylalanyl-tRNA synthetase in the presence of AMP and PP_i was measured by essentially the same method as described for the hydrolysis. [^{14}C]Phe-$tRNA^{Phe}$ (10 μCi/μmol, 90% charged) was in excess over the enzyme. Reaction volumes were 3 mL (25 °C). Samples of 80 μL were drawn at varying times. Rates of deacylation were computed from the appearance of radioactivity in the supernatant after correction for spontaneous hydrolysis. Rate constants were then calculated on the basis of enzyme concentrations. [^{14}C]Phe-$tRNA^{Phe}_{h\nu}$ (84 μCi/μmol, 30% charged) was less than the enzyme (in at least 5-fold excess) and yielded 700–1000 cpm in the supernatant after complete deacylation. Radioactivity was evaluated as first-order plots. Deacylation rate constants were computed from the slopes of the best linear fits.

The kinetics of the association of Phe-$tRNA^{Phe}_{h\nu}$ and enzyme to form reversible complexes were measured by rapid mixing of the reactants in a Durrum stopped-flow apparatus equipped for fluorescence detection (Pimmer & Holler, 1979). The fluorescence emission of an added reporter group, 2-(*p*-toluidinyl)naphthalene-6-sulfonate, was exploited, as has been described in detail (Kosakowski & Holler, 1973; Bartmann et al., 1975b; Güntner & Holler, 1979; Holler, 1980). The intrinsic kinetics of enzyme·TNS complex formation do not interfere with kinetics observed here (Holler, 1980).

The equilibrium formation of the enzyme·$tRNA^{Phe}_{h\nu}$ complex was studied by titration experiments observing the protein intrinsic fluorescence at 340 nm (excitation wavelength 300 nm). A description of this technique together with appropriate corrections for absorption by tRNA has been given (Holler et al., 1980).

The kinetics of the UV-induced cross-linking of tRNA or its derivatives between the bases in positions 8 and 13 were measured as described (Favre et al., 1979). Reaction solutions of 500 μL contained 50 mM Tris-HCl buffer (pH 7.5), 10 mM $MgCl_2$, 0.1 mM EDTA, 0.4 mM dithioerythritol, and either $tRNA^{Phe}$, $tRNA^{Phe}_{HNO_2}$, Phe(OH)-$tRNA^{Phe}_{HNO_2}$ (80%) charged) at 5 A_{260}/units/mL or the same compounds plus 7 μM phenylalanyl-tRNA synthetase. For comparison, pairs of solutions were irradiated together at 15 °C. Samples of 50 μL were drawn over a period of 40 min. Completeness of the reaction was achieved by increasing the light flux and continuing the irradiation for an additional 30 min. Each sample was diluted by 500 μL of water. A total of 50 μL of 1 M NH_3 in water was added, followed by 50 μL of 2 M $NaBH_4$ in 0.2 M aqueous NH_3. Reduction was allowed overnight in a dark place. A total of 200 μL of 1 M sodium acetate, pH 5, was added and the fluorescence intensity measured at 451 nm (excitation wavelength 390 nm) in a Hitachi Perkin-Elmer Model MPF-2A fluorimeter. At the end of the irradiation, the fraction of [^{14}C]Phe(OH)-$tRNA^{Phe}_{HNO_2}$ was determined on DEAE-cellulose filter disks (Santi & Anderson, 1974) to be 65% of the total $tRNA^{Phe}_{HNO_2}$ in the absence and 40% in the presence of enzyme. When the kinetics of cross-linking of native $tRNA^{Phe}$ and Phe-$tRNA^{Phe}$ were to be compared, two 1-mL samples containing 50 mM Tris-HCl buffer (pH 7.5), 12 mM $MgCl_2$, 0.1 mM EDTA, 0.4 mM dithioerythritol, 5 A_{260} units/mL $tRNA^{Phe}$, 25 μM [^{14}C]Phe (10 μCi/μmol), 2 mM ATP, and 10 μg of inorganic pyrophosphatase were simultaneously irradiated. To one sample 3 nM and in another run 0.4 μM phenylalanyl-tRNA synthetase were added; to the other sample, corresponding amounts (by weight) of bovine serum albumin were added. Samples of 50 μL were drawn for the fluorimetric analysis and 20 μL for the DEAE-cellulose filter assay of [^{14}C]Phe-$tRNA^{Phe}$. In the case of low enzyme concentration, maximum charging was 55% at the beginning of irradiation and 50% at the time when 50% of the total $tRNA^{Phe}$ was cross-linked. In the case of high enzyme concentration, it was 100% charging at the beginning and 90% at the time when 50% cross-linking was observed.

Results

Effect of Cross-Linking on the Steady-State Rate of tRNA Phenylalanylation. When during the course of irradiation a

[1] Abbreviations used: EDTA, (ethylenedinitrilo)tetraacetic acid; Tris, 2-amino-2-(hydroxymethyl)-1,3-propanediol; TNS, 2-(*p*-toluidinyl)-naphthalene-6-sulfonate; Phe-$tRNA^{Phe}$, L-phenylalanyl ester of $tRNA^{Phe}$; $tRNA^{Phe}_{h\nu}$, $tRNA^{Phe}$ cross-linked between bases in positions 8 and 13; $tRNA^{Phe}_{HNO_2}$, $tRNA^{Phe}$ after treatment with nitrous acid; Phe(OH)-$tRNA^{Phe}_{HNO_2}$, DL-β-phenyllactyl ester of $tRNA^{Phe}_{HNO_2}$; Phe-$tRNA^{Phe}_{h\nu}$, L-phenylalanyl ester of $tRNA^{Phe}_{h\nu}$.

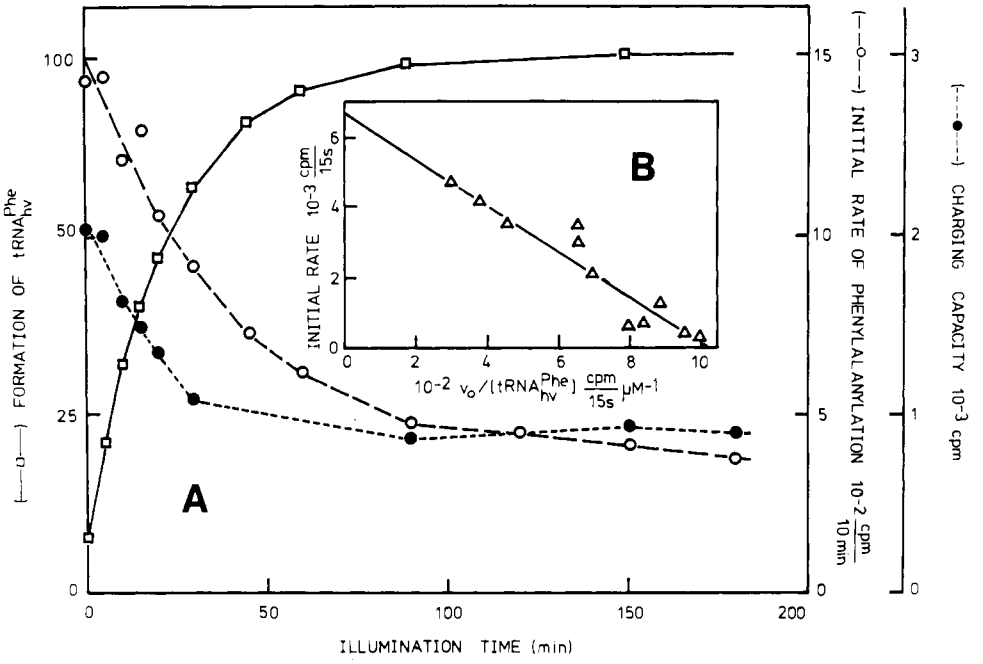

FIGURE 1: Rate of phenylalanylation, charging capacity, and amounts of cross-link formation of tRNA^{Phe} as a function of irradiation time. Solutions contained 10 A_{260} units of tRNA^{Phe}/mL (initially a charging capacity of 1100 pmol/A_{260} unit), 50 mM Tris-HCl buffer (pH 7.5), 10 mM $MgCl_2$, 0.1 mM EDTA, and 0.4 mM dithioerythritol. Irradiation was carried out at 13 °C as has been described (Favre et al., 1979). At times indicated in panel A, aliquots of 0.2 A_{260} unit were analyzed for the amounts of cross-link formed and for the rate of enzymatic phenylalanylation (10-min reaction time, 0.17 nM phenylalanyl-tRNA synthetase). Aliquots of 0.1 A_{260} were used to determine the charging capacity (13 nM synthetase). Steady-state kinetic parameters of phenylalanylation of fully cross-linked tRNA^{Phe} were obtained for 33 nM synthetase and 15-s reaction time from acid precipitable radioactivity that had been plotted according to Eadie (1942) in (B). Counting efficiency was 90%.

sample of tRNA^{Phe} was assayed for initial rates of aminoacylation (using a standard concentration of 1 μM), a continuous decrease of the rate was observed, arriving eventually at a final plateau (Figure 1A). The reason for the inhibition by irradiation was established by the determination of the Michaelis–Menten constant: K_m = 6.3 ± 1 μM for fully cross-linked tRNA^{Phe} as opposed to K_m = 0.26 μM (Stuhlberg, 1967) for native tRNA^{Phe} (Figure 1B). The catalytic rate constant calculated from the maximum rate was 2.6 ± 0.3 s^{-1}, in comparison with 2.7 ± 0.3 s^{-1} for native tRNA^{Phe} under identical conditions.

Effect of Cross-Linking on the Phenylalanylation Capacity of tRNA. The degree of cross-linking was measured by the sodium borohydride method, and the charging capacity for phenylalanylation was followed in the presence of a relatively low concentration of enzyme, both as a function of time (Figure 1A). The charging capacity decreased while, in a kind of mirror image, the level of cross-linked tRNA increased. The discrepancy between the charging levels of native and cross-linked tRNA^{Phe} was observed to be a function of enzyme concentration, as has been reported (Dietrich et al., 1976). Maximum charging was 75% of that obtained before irradiation (0.3 μM enzyme and tRNA, respectively). The discrepancy observed in Figure 1 is mainly the consequence of relatively weak binding of substrate tRNA$_{hv}^{Phe}$ and strong binding of product Phe-tRNA$_{hv}^{Phe}$, as will be seen from subsequent results.

Kinetics of Enzymatic Hydrolysis of Phe-tRNA$_{hv}^{Phe}$ in the Absence of AMP and PP_i. Hydrolysis was measured as a function of time at varying fixed concentrations of enzyme in a 5-fold or higher excess over Phe-tRNA$_{hv}^{Phe}$. An excess of enzyme eliminates possible product inhibition by tRNA$_{hv}^{Phe}$. Initial rates of hydrolysis corrected for spontaneous hydrolysis are given in Figure 2 as a function of enzyme concentration. The rates approach a saturation plateau at concentrations not expected on the basis of the K_m value that had been measured

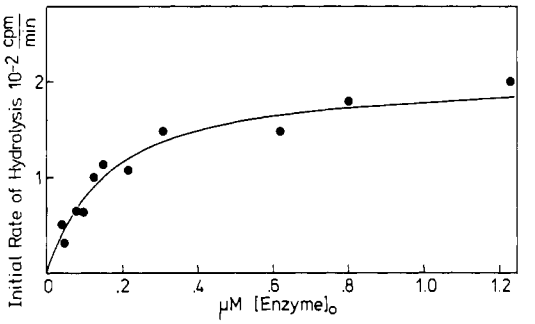

FIGURE 2: AMP-independent deacylation (hydrolysis) of Phe-tRNA$_{hv}^{Phe}$. Conditions (25 °C) were 50 mM Tris-HCl buffer (pH 7.5), 0.2 mM EDTA, 0.4 mM dithioerythritol, 10 mM $MgCl_2$, and phenylalanyl-tRNA synthetase in at least 4-fold excess over Phe-tRNA$_{hv}^{Phe}$ (20 μCi/μmol, 0.01–0.2 μM). Initial rates were determined from plots of radioactivity in the supernatant (see Materials and Methods) vs. time. The drawn curve is calculated for maximum rate = 210 cpm/min and K_m = 0.16 μM on the basis of enzyme concentration.

for the enzymatic aminoacylation (Figure 1B). Kinetic parameters were evaluated according to Eadie (1942), K_m (hydrolysis) = 0.32 ± 0.05 μM and k_{cat} (hydrolysis) = 0.013 ± 0.002 s^{-1}. The value of the Michaelis–Menten constant was obtained on the basis of active site concentrations (2 active sites/enzyme molecule; Bartmann et al., 1975a). Interference with hydrolysis of possible residual native Phe-tRNA^{Phe} as an impurity could be ruled out by finding linear first-order plots over more than 90% Phe-tRNA$_{hv}^{Phe}$ hydrolyzed in a complete time dependence.

The effect of added Phe on the kinetics of hydrolysis was studied under conditions of 0.15 μM Phe-tRNA$_{hv}^{Phe}$ and 0.8 μM phenylalanyl-tRNA synthetase in the presence or absence of 5 mM Phe (the dissociation constant of the enzyme-Phe complex is 30 μM; Bartmann et al., 1975b). Measured rate constants were 0.011 s^{-1} in the presence and 0.012 s^{-1} in the absence of Phe.

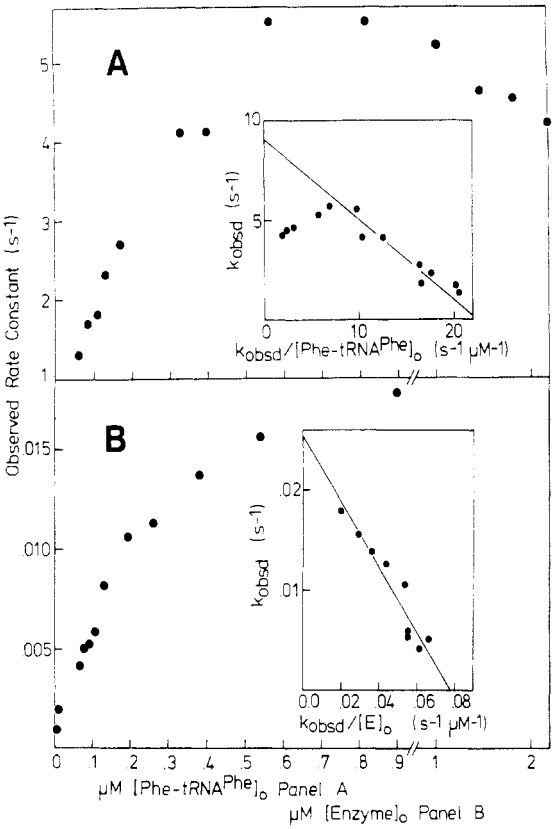

FIGURE 3: AMP-dependent deacylation (reverse of phenylalanylation) of native and cross-linked Phe-tRNA. (Panel A) Native Phe-tRNA. (Panel B) Cross-linked Phe-tRNA. Conditions (25 °C) were 50 mM Tris-HCl buffer (pH 7.5), 0.2 mM EDTA, 0.4 mM dithioerythritol, 10 mM $MgCl_2$, 2 mM AMP, 10 mM $MgPP_i$, and 70 pM phenylalanyl-tRNA synthetase in panel A or enzyme in at least 5-fold excess over Phe-tRNA in panel B. Deacylation rate constants were evaluated either from initial rates (for panel A) or from first-order plots (for panel B). Kinetic parameters were calculated from linearized plots according to Eadie (1942) in the figure insets.

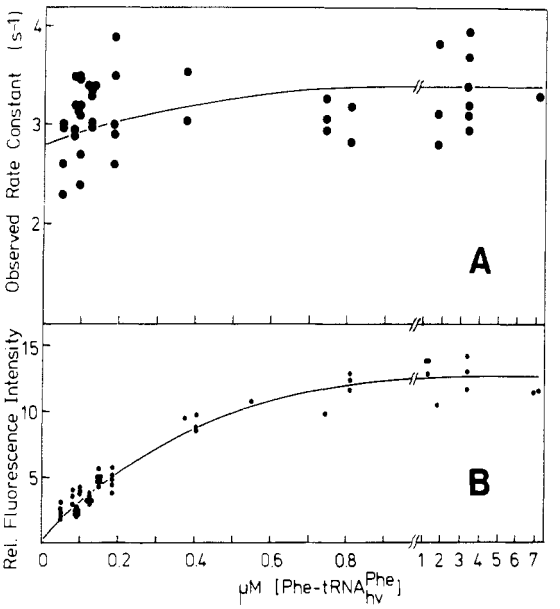

FIGURE 4: (Panel A) Formation of enzyme·Phe-$tRNA^{Phe}_{hv}$ complex. Rate constants of complex formation were measured by observation of the intensity of the fluorescence emitted by TNS bound to the Phe-specific site of the enzyme (Kosakowski & Holler, 1973). When Phe-tRNA occupies this site, TNS can no longer bind and becomes almost nonfluorescent. The techniques have been described in detail (Holler, 1980). Conditions (25 °C) were 50 mM Tris-HCl buffer (pH 7.5), 0.1 mM EDTA, 0.2 mM dithioerythritol, 10 mM $MgCl_2$, 6 μM TNS, and phenylalanyl-tRNA synthetase (0.02–0.08 μM). The preparation of Phe-$tRNA^{Phe}_{hv}$ and the stopped-flow apparatus used were exactly the same as described (Güntner & Holler, 1979). (Panel B) Formation of the enzyme·Phe-$tRNA^{Phe}_{hv}$ complex measured via the decrease in fluorescence intensity of TNS at equilibrium. The same reactions as those under panel A have been observed after they had approached completion. Relative intensity differences have been normalized to that seen after mixing enzyme against L-phenylalanine (5 mM final concentration) both in the presence of TNS. Drawn curves have been computed on the basis of kinetic constants in Table II.

AMP-Dependent Deacylation of Phe-$tRNA^{Phe}_{hv}$. Deacylation was measured in the presence of almost saturating concentrations of AMP (K_m = 0.24 mM at 1 mM $MgCl_2$; Bartmann et al., 1975b) and $MgPP_i$ (K_m = 0.14 mM; Pimmer & Holler, 1979) and with Phe-$tRNA^{Phe}$ in excess over enzyme (Figure 3A) or with Phe-$tRNA^{Phe}_{hv}$ in stoichiometric ratios below enzyme (Figure 3B). Rate constants for the native tRNA are much higher than those for the cross-linked tRNA. Kinetics are biphasic in the case of Phe-$tRNA^{Phe}$, showing decreased rates at concentrations above 1 μM. Experiments at Phe-$tRNA^{Phe}_{hv}$ of 1–5 μM (in excess over 80 nM enzyme), however, did not reveal a decrease in the value of the rate constant, 0.025 ± 0.005 s^{-1} (data not shown). The maximum rate constant from the dependence where enzyme is in excess over Phe-$tRNA^{Phe}_{hv}$ (Figure 3B) gives a value of 0.025 ± 0.002 s^{-1}. The value of the Michaelis–Menten constant was calculated from the linearized plot (Eadie, 1942) in Figure 3B, inset, to be 0.33 ± 0.03 μM on the basis of the concentration of the enzyme rather than on the basis of the concentration of the active sites. The reason is that in the presence of almost saturating AMP and PP_i the enzyme is expected to have dissimilar active sites with only one of them carrying the reactants. Although not for AMP and PP_i, anticooperative binding has been reported for all the other reactants and Mg^{2+} (Pimmer & Holler, 1979). The kinetic data have been summarized in Table I.

The rates of AMP-dependent deacylation are marginal in the case of Phe-$tRNA^{Phe}_{hv}$. They have not been corrected for enzymatic hydrolysis (spontaneous hydrolysis is mostly negligible under the conditions used). In fact, the rates observed here are comparable with those of enzymatic hydrolysis (Figure 2). It had to be established as to what degree the two types of reactions occur side by side. To this end, a mixture of 26 μM enzyme, 25 μM Phe-$tRNA^{Phe}_{hv}$, 2 mM [^{14}C]AMP (572 μCi/μmol), 3 mM PP_i, 15 mM $MgCl_2$, 100 mM Tris-HCl buffer (pH 7.5), 0.2 mM EDTA, and 0.4 mM dithioerythritol in a volume of 20 μL was reacted for 15 min at 25 °C. The reaction was stopped in ice by addition of 200 μL of 0.1 M sodium acetate buffer, pH 4.5. The mixture was applied to a 0.5 × 4.5 cm DEAE-Sephadex A-25 column at 4 °C. [^{14}C]AMP was removed by washing the column with 40 mL of 0.1 M sodium acetate buffer. Elution of [^{14}C]ATP was followed in the presence of 0.5 M sodium acetate. After correction for counting efficiency, the total amount of radioactivity for [^{14}C]ATP was found to be 30% of the Phe-$tRNA^{Phe}_{hv}$ deacylated. Thus, hydrolysis accounts for 70% deacylation. Regarding error limits, an appropriate estimate for the catalytic rate constant for AMP-dependent deacylation is 0.01 s^{-1}.

Enzyme·$tRNA^{Phe}_{hv}$ Complex. The measurement of the enzyme's (0.1–0.5 μM) intrinsic fluorescence as a function of $tRNA^{Phe}_{hv}$ concentration did not reveal a distinct change (after correction for tRNA absorbance) below 1 μM in contrast to titration with native $tRNA^{Phe}$ (Bartmann et al., 1975a). At higher concentrations up to 8–10 μM $tRNA^{Phe}_{hv}$, a 10–15% decrease of the fluorescence intensity became apparent (data

Table I: Kinetic and Equilibrium Constants of Phenylalanyl-tRNA Synthetase Reactions

reaction	K_{diss} (μM)	K_m (μM)	k_{cat} (s^{-1})
enzyme·tRNA^{Phe} complex	0.2[a]		
enzyme·tRNA$^{Phe}_{h\nu}$ complex	2–5 5 ± 3[b]		
phenylalanylation,			
tRNA^{Phe}		0.26[c]	3.8 ± 0.3[d]
tRNA$^{Phe}_{h\nu}$		6.3 ± 0.1	3.6 ± 0.3[e]
AMP-dependent deacylation, Phe-tRNA^{Phe}		0.4 ± 0.06	9 ± 1
Phe-tRNA$^{Phe}_{h\nu}$		0.33 ± 0.03	0.01
AMP-independent deacylation, Phe-tRNA^{Phe}		0.11[f]	0.007 ± 0.002[f]
Phe-tRNA$^{Phe}_{h\nu}$		0.32 ± 0.05	0.013 ± 0.002

[a] Bartmann et al. (1975a). [b] Holler et al. (1980). [c] Stuhlberg (1967). [d] Holler (1980). [e] Calculated on the basis of the experimental value 2.6 s^{-1} (Figure 1B) for saturation concentrations of Phe and ATP by using K_m values of 5 μM and 0.2 mM, respectively (Holler & Kosakowski, 1973). [f] Güntner & Holler (1979). Conditions refer to 50–100 mM Tris-HCl buffer (pH 7.5) and 10 mM Mg^{2+} and 25–28 °C.

Table II: Kinetic Parameters of Enzyme·Phe-tRNA Complexes[a]

Phe-tRNA	k_b (s^{-1})	k_f (μM^{-1} s^{-1})	Phe-specific site $K^{(2)}_{diss} = k_b/k_f$ (μM)	tRNA-specific site $K^{(1)}_{diss}$ (μM)
cross-linked (Phe-tRNA$^{Phe}_{h\nu}$)	2.9 ± 0.3	1.3 ± 0.3	2.2 ± 0.3	0.35 ± 0.05
native[b] (Phe-tRNA^{Phe})	3 ± 0.2	32 ± 5	0.09 ± 0.01	0.4 ± 0.01

[a] Conditions were 50 mM Tris-HCl buffer (pH 7.5), 10 mM $MgCl_2$, 0.1 mM EDTA, and 0.2 mM dithioerythritol at 25 °C. [b] Holler (1980).

not shown). K_{diss} values between 2 and 5 μM were estimated. The accuracy of the measurement was limited by the high absorbance of the tRNA.

Enzyme·Phe-tRNA$^{Phe}_{h\nu}$ Complexes. The formation of enzyme·Phe-tRNA$^{Phe}_{h\nu}$ complexes when enzyme and Phe-tRNA$^{Phe}_{h\nu}$ were rapidly mixted in a stopped-flow apparatus was followed via a decrease in the fluorescence intensity of added TNS. The time dependence was found to be first order. The dependence of the observed rate constants, k_{obsd}, on the concentration of Phe-tRNA$^{Phe}_{h\nu}$ (in a higher than 5-fold excess over enzyme) is given in Figure 4A. The reaction amplitude at equilibrium is shown as a function of concentration in Figure 4B. In spite of considerable scattering, a marginal dependence of k_{obsd} is seen in Figure 4A. A similar observation, though considerably more pronounced, has been reported for the association kinetics of Phe-tRNA^{Phe} (Holler, 1980).

We have shown that aminoacyl-tRNA can associate with phenylalanyl-tRNA synthetase via a binding site that is specific for tRNA^{Phe} and a second site that involves the phenylalanine-specific binding site (Güntner & Holler, 1979). Acyl-tRNA can bind to one site at a time but not to both sites simultaneously. In the absence of Phe or acyl-tRNA, the added indicator TNS occupies a fraction of enzyme at the Phe-specific site and thereby gains a large increase in the intensity of its fluorescence (Kosakowski & Holler, 1973). However, when upon mixing this site is taken by an acyl-tRNA, the indicator is displaced into the solvent and its fluorescence almost extinguished (Güntner & Holler, 1979). Thus, fluorescence intensity changes of TNS reflect a combination of interactions of an acyl-tRNA with the two binding sites of the enzyme.

Stopped-flow kinetics for the formation of enzyme·Phe-tRNA^{Phe} complexes have been analyzed to resemble a superposition of two association reactions which occur in parallel (Holler, 1980). In analogy, the present kinetics will be handled according to eq 1 and 2. The symbol L stands for Phe-tRNA$^{Phe}_{h\nu}$. Rate constants k_f and k_b refer to association and dissociation, respectively. Reaction 1 is fast. It resembles binding to the tRNA-specific site of the enzyme. Reaction 2 is the association of Phe-tRNA$^{Phe}_{h\nu}$ with the Phe-specific site. $(EL)_1$ and $(EL)_2$ are the corresponding complexes. Comparison of the intensity change observed at equilibrium with the change seen after completion of the stopped-flow reaction shows no difference. Hence, the decrease in intensity is caused by reaction 2, exactly as in the case of Phe-tRNA^{Phe} (Holler, 1980). In this case, an equation has been derived for the observed rate constant, k_{obsd}, as a function of the concentration of L:

$$E + L \underset{}{\overset{\text{fast}}{\rightleftharpoons}} (EL)_1 \quad (1)$$

$$E + L \underset{k_b}{\overset{k_f}{\rightleftharpoons}} (EL)_2 \quad (2)$$

$$k_{obsd} = k_b + k_f K^{(1)}_{diss} \frac{[L]}{K^{(1)}_{diss} + [L]} \quad (3)$$

The dissociation constant refers to reaction 1:

$$K^{(1)}_{diss} = \frac{[E][L]}{[(EL)_1]}$$

It is assumed that initial concentrations are $[L] \gg [E]_0$. The values of k_b, k_f, and $K^{(1)}_{diss}$ can be calculated from the results in Figure 4A,B, as will be shown. From Figure 4A, one obtains with eq 3 at high concentrations of $[L] \gg K^{(1)}_{diss}$

$$k_{obsd}(max) = k_b + k_f K^{(1)}_{diss} \quad (4)$$

The dependence of the change in fluorescence intensity on [L] (Figure 4B) can be treated in analogy to nonproductive binding (Rupley & Gates, 1967). Here, this type of binding is identified with reaction 1, which does not cause the intensity change. It follows for the apparent dissociation constant that is evaluated from the concentration dependence in Figure 4B by conventional procedures [see, for instance, Güntner & Holler (1979)]

$$\frac{1}{K_{diss}(app)} = \frac{k_f}{k_b} + \frac{1}{K^{(1)}_{diss}} \quad (5)$$

By the same means, one derives an expression for ΔF_{max} (eq 6), the decrease of intensity at saturation concentration of L.

$$\frac{\Delta F_{max}}{\Delta F_{Phe \to \infty}} = \left[1 + \frac{1}{K^{(1)}_{diss}} \frac{k_b}{k_f} \right]^{-1} \quad (6)$$

$\Delta F_{Phe \to \infty}$ refers to the intensity decrease if there would be no nonproductive binding. The value of ΔF_{max} was obtained from the data in Figure 4, the value of $\Delta F_{Phe \to \infty}$ in an experiment where 5 mM Phe was added instead of L.

From combinations of eq 4–6, eq 7 and 8

$$\Delta F_{max}/\Delta F_{Phe \to \infty} = K_{diss}(app)\frac{k_f}{k_b} \quad (7)$$

$$k_b = k_{max}[1 - \Delta F_{max}/\Delta F_{Phe\rightarrow\infty}] \quad (8)$$

were calculated. With the experimental values $k_{max} = 3.3 \pm 0.3\ s^{-1}$, $K_{diss}(app) = 0.3 \pm 0.05\ \mu M$, and $\Delta F_{max}/\Delta F_{phe\rightarrow\infty} = 0.13 \pm 0.02$, the values for the parameters k_b, k_f, and $K_{diss}^{(1)}$ were computed from eq 4, 7, and 8 and are listed in Table II. The value of the dissociation constant of the $(EL)_2$ complex is calculated to be $k_b/k_f = 2.2 \pm 0.3\ \mu M$, in contrast to $0.35 \pm 0.05\ \mu M$ for the dissociation constant of $(EL)_1$.

Effect of Charging on the Rate of UV-Induced Cross-Linking of tRNA^{Phe}. The photoreaction kinetics of cross-linking have been determined on the unacylated and acylated $tRNA^{Phe}$, before and after treatment with HNO_2, and either in the presence or absence of the cognate synthetase (in excess over tRNA). The relative rate constants are compared in Table III. Relative yields are of the same magnitude and, where they were less than unity, cannot be responsible for the effects observed on the relative rates. Formation of enzyme complexes leads to protection of tRNA regardless of whether it is native or HNO_2 treated, acylated or unacylated. The effect of phenylalanylation in the case of native tRNA is marginal whereas rates show a definite decrease after acylation of HNO_2-treated tRNA. In conclusion, it appears as if HNO_2 treatment has led to or augmented the effect of acylation on some structural rearrangement within the tRNA that is seen in terms of protection.

Discussion

Why Conformers? There is accumulating evidence that tRNA in solution exists in more than one interconvertable conformation [Crothers & Cole (1978) and references therein]. We have observed by circular dichroism and UV-induced cross-linking (the same technique as applied in the present work) that $tRNA^{Phe}$ exhibits a new conformation when associating with phenylalanyl-tRNA synthetase of *E. coli* (Favre et al., 1979). Although we cannot rule out a synthetase-induced conformation, as we have called it, the results can be explained equally well as a preferred binding of a tRNA conformer in equilibrium with other conformers.

Present reasons for introducing the concept of tRNA conformers are the following: (a) Nitrous acid treated $tRNA^{Phe}$ (Güntner & Holler, 1979) and native $tRNA^{Phe}$ have identical rates of UV-induced cross-linking (Table III). However, DL-β-phenyllactyl-$tRNA^{Phe}_{HNO_2}$ reacts at a slower rate (Table III). β-Phenyllactylation may be assumed to cause a rearrangement that favors a less UV-reactive tRNA species. (b) According to the three-dimensional structure of yeast $tRNA^{Phe}$, a direct steric or electronic interference between the site of UV cross-link and the site of phenylalanylation is ruled out (Kim et al., 1973). Thus, the equilibrium constants (eq 9)

$$K_{eq} = \frac{[AMP][PP_i][Phe\text{-}tRNA]}{[ATP][Phe][tRNA]} \quad (9)$$

should be identical for native and cross-linked tRNA. The values of K_{eq} can be calculated from the values of the Michaelis–Menten constants K_m(ATP), K_m(Phe), K_m(tRNA), K_m(AMP), $K_m(PP_i)$, and K_m(Phe-tRNA) and the values of the catalytic rate constants k_{cat}(phenylalanylation) and k_{cat}(AMP-dependent deacylation) (Haldane, 1930). In the concentration range of interest, K_m values and K_{diss} values do not indicate substantial coupling between Michaelis–Menten constants for tRNA or Phe-tRNA and the small reactants that would be different for native and cross-linked tRNA (Tables I and II; Bartmann et al., 1975a; Pimmer & Holler, 1979). For this reason, comparison of the phenylalanylation equilibria is based on the reduced form of the equilibrium constant (eq 10). The values of K_{eq}' are 0.6 for native $tRNA^{Phe}$ and 19

$$K_{eq}' = \frac{k_{cat}(\text{aminoacylation})}{K_m(\text{tRNA})} \frac{K_m(\text{Phe-tRNA})}{k_{cat}(\text{deacylation})} \quad (10)$$

for cross-linked $tRNA^{Phe}$ as calculated from numbers listed in Table I. The 31-fold difference indicates to us that phenylalanylation of $tRNA^{Phe}_{h\nu}$ is energetically favored over that of $tRNA^{Phe}$. We conclude that this energy is derived from a rearrangement of $tRNA^{Phe}_{h\nu}$ after it has become aminoacylated. In the following discussion, we will present evidence that the differences between kinetic and equilibrium constants for the reaction of native and cross-linked $tRNA^{Phe}$ are satisfactorily explained on the basis of tRNA conformers in equilibrium.

Table III: UV-Induced Cross-Linking of Native and Modified $tRNA^{Phe}$[a]

condition	relative rate	relative yield
$tRNA^{Phe}$	1.0	1.0
$tRNA^{Phe}$ + enzyme[b]	0.4–0.5	1.0
Phe-$tRNA^{Phe}$[c]	0.9	1.0
$tRNA^{Phe}_{HNO_2}$	1.0	1.0
$tRNA^{Phe}_{HNO_2}$ + enzyme	0.25	0.85
DL-β-phenyllactyl-$tRNA^{Phe}_{HNO_2}$	0.55	1.1
DL-β-phenyllactyl-$tRNA^{Phe}_{HNO_2}$ + enzyme	0.18	0.88

[a] Concentrations of enzyme and tRNA were 7 and 6.5 μM tRNA, respectively. Rate constants were evaluated from first-order plots of log $(F_\infty - F_t)$ vs. time (F_t = fluorescence intensity after sodium borohydride reduction at time t, F_∞ = intensity at infinite time). Experimental errors are of the order of 10%. [b] Favre et al. (1979). [c] For conditions, see text.

Strategy. Assume that tRNA or Phe-tRNA exists in at least two forms in rapid equilibrium (eq 11) and that one of

$$T_1 \rightleftharpoons T_2 \quad (11)$$

them, for example, T_1, is reactive. In the case of formation of the enzyme-tRNA complex, the concentration $[ET_1]$ is given by eq 12. If $K_c = [T_1]/[T_2]$ is the conformer equilibrium

$$[ET_1] = \frac{[T_1][E]}{K_{diss}(\text{true})} \quad (12)$$

constant and $[T]_0 = [T_1] + [T_2]$ the total concentration of tRNA ($[ET_1]$ negligible), then

$$[ET_1] = [E][T]_0 \frac{K_c}{K_{diss}(\text{true})(1 + K_c)} \quad (13)$$

and the apparent dissociation constant

$$K_{diss}(app) = K_{diss}(\text{true}) \frac{1 + K_c}{K_c} \quad (14)$$

If the apparent dissociation constants for native (1) and cross-linked tRNA (2) complexes are to be compared and if the only difference between the two were the concentration of conformers, the ratio of eq 15 could be used as a correction

$$\frac{K_{diss}(app)(2)}{K_{diss}(app)(1)} = \frac{\dfrac{K_{c2} + 1}{K_{c2}}}{\dfrac{K_{c1} + 1}{K_{c1}}} = F_{cor} \quad (15)$$

factor if, for instance, rate constants are to be compared. From

a comparison of cross-linking rates of tRNA^{Phe} and Phe-tRNA^{Phe} (Table III), we learn that the population of these tRNAs consists largely of the same species with respect to cross-linking whereas this is not the case of HNO_2-modified Phe-tRNA^{Phe}. Evidently, in this latter example, the conformer equilibrium constant may have been changed upon acylation. Under the assumption that different conformers have different dissociation constants for their enzyme complexes, correction factors like eq 15 may be used to deduce the value of the rate constant of cross-linking of DL-β-phenyllactyl-tRNA$^{Phe}_{HNO_2}$ from that of cross-linking of tRNA$^{Phe}_{HNO_2}$.

The strategy will be used to demonstrate a redistribution of conformers on cross-linking of tRNA^{Phe} and on phenylalanylation of tRNA$^{Phe}_{h\nu}$. The strategy is supported by the finding of a unique mechanism of enzyme reactions of both native and cross-linked tRNA^{Phe} if correction is made for the conformer equilibria.

Phenylalanylation. Both native and cross-linked tRNA^{Phe} are phenylalanylated with almost identical catalytic rate constants yet with 24-fold different values of the Michaelis–Menten constants (Table I). The same difference is mirrored by the values of the dissociation constants of the enzyme·tRNA complexes (Table I). In the context of eq 11, we may say that tRNA form T_2 does not bind to the enzyme. UV-induced cross-linking has shifted the equilibrium toward this form. The factor α, by which the value of K_c has been decreased, can be calculated on the basis of eq 15 and setting $K_{c2} = \alpha K_c$

$$\frac{K_{diss}(app)(2)}{K_{diss}(app)(1)} = \frac{1 + \alpha K_c}{\alpha(1 + K_c)} \qquad (16)$$

In the present case, we obtain $\alpha = (25 + 24K_c)^{-1}$. No information on the value of K_c is available. If $K_c = 9$ (90% tRNA^{Phe} is conformer T_1), α will be 241^{-1}; if $K_c = 1$ (equal amounts of conformers T_1 and T_2), $\alpha = 50^{-1}$. Even though K_c can be arbitrarily small, α never exceeds 25^{-1}. This demonstrates why, if K_c is large, a fixed amount of free energy (corresponding to a fixed value α) does barely show up as a shift in properties, K_{diss}(app), while the same amount of free energy has a pronounced effect if K_c is small. This may explain why some modifications of tRNA, for instance aminoacylation, would show up only in combination with others, for instance HNO_2 treatment (Table III), which provide a shift of K_c from high to low values.

We have found that the rate of UV-induced cross-linking is reduced in the presence of enzyme·tRNA^{Phe} complex formation (Favre et al., 1979). Accordingly, we may assume that the nonbinding conformer T_2 is the one which is rapidly cross-linked.

AMP-Dependent Deacylation. The effect of cross-linking on phenylalanylation is to enhance the K_m value of tRNA$^{Phe}_{h\nu}$ in comparison to that of tRNA^{Phe} (Table I). In contrast, the effect on the reverse reaction is to decrease the catalytic rate constant 10^3-fold with respect to k_{cat} of Phe-tRNA^{Phe} (Table I). We shall see that the different effects are explained by action of cross-linking and phenylalanylation on the equilibria of tRNA conformers.

For phenylalanylation, the similarity of k_{cat} values (Table I) suggests the rate-limiting step for native and cross-linked tRNA to be identical. It has been proposed that the rate-limiting steps of both phenylalanylation and AMP-dependent deacylation are a conformational change during dissociation–association of enzyme·Phe-tRNA, involving the Phe-specific binding site of the enzyme (Holler, 1976, 1980; Güntner & Holler, 1979). By employing the TNS method (Holler, 1980), the kinetics of complex formation can be measured. For Phe-tRNA$^{Phe}_{h\nu}$, results are shown in Figure 4A,B. The kinetic parameters are compared with those for Phe-tRNA^{Phe} in Table II. (1) The dissociation constants $K^{(1)}_{diss}$ that are attributed to rapidly forming complexes at the tRNA-specific site of the enzyme have almost identical values for native and cross-linked Phe-tRNA. They agree with the K_m values for deacylation (Table I). (2) The dissociation rate constants k_b for the complex at the Phe-specific site of the enzyme have values which are identical for both Phe-tRNAs within experimental error and which, as indicated by the proposal, are in agreement with the k_{cat} values of phenylalanylation (Table I). (3) The second-order association rate constants k_f are different for native and cross-linked tRNA. In order to be compared with the k_{cat} values of AMP-dependent deacylation, they have to be transformed into first-order rate constants, k_f(1st), by multiplication with the values $K^{(1)}_{diss}$ (see eq 3). The values are then k_f(st) = 12.6 s^{-1} for native and 0.46 s^{-1} for cross-linked Phe-tRNA.

The stopped-flow kinetic parameters of formation of the enzyme·Phe-tRNA complexes are first considered in the light of the concept of tRNA conformers before we continue with their implication in AMP-dependent deacylation. First, we observe that the value k_f is reduced 25-fold for cross-linked Phe-tRNA when compared with that of native Phe-tRNA. This can be explained by the same redistribution of conformers upon cross-linking as has been discussed for the binding of tRNA$^{Phe}_{h\nu}$. When the value $k_f = 1.3\ \mu M^{-1}\ s^{-1}$ (Table II) is multiplied with the correction factor $F_{cor} = K_{diss}$(tRNA$^{Phe}_{h\nu}$)/K_{diss}(tRNA^{Phe}) = 25 (Table I), indeed the value $k_f = 32\ \mu M^{-1}\ s^{-1}$ for native Phe-tRNA is obtained. In conclusion, cross-linking favors a conformer of Phe-tRNA that does not bind to the Phe-specific site of the enzyme. Second, the dissociation constant $K^{(1)}_{diss}$ for the complex at the tRNA-specific site has a smaller value for Phe-tRNA$^{Phe}_{h\nu}$ than for tRNA$^{Phe}_{h\nu}$ (Tables I and II). This cannot be accounted for by an interaction between the phenylalanyl moiety and the Phe-specific binding site. An unspecific interaction with the enzyme surface cannot be excluded, although such an interaction has not been observed for Phe-tRNA^{Phe} and other cases (Güntner & Holler, 1979); it seems thus unlikely. In conclusion, the concentration of conformers of tRNA$^{Phe}_{h\nu}$ that bind to the tRNA-specific site is thought to be enhanced by phenylalanylation. This specific effect, which excludes the Phe-specific binding site, is accounted for by an extension of reaction eq 11. T_1 and T_2 conformers have appeared upon

$$\begin{array}{ccc} T_1 & \rightleftharpoons & T_2 \\ \Updownarrow & & \Updownarrow \\ T_1' & \rightleftharpoons & T_2' \end{array} \qquad \begin{array}{l} K_c = \dfrac{[T_1]}{[T_2]} = \dfrac{[T_1']}{[T_2']} \\ \\ K_{c'} = \dfrac{[T_1]}{[T_1']} = \dfrac{[T_2]}{[T_2']} \end{array} \qquad (17)$$

cross-linking and T_1' and T_2' upon phenylalanylation of cross-linked tRNA^{Phe}. We tentatively infer that conformers T_1 and T_1' bind to the Phe-specific site and conformers T_1, T_1', and T_2' to the tRNA-specific site of the enzyme. This effect of phenylalanylation causes a 14-fold decrease in the value of the dissociation constant when tRNA$^{Phe}_{h\nu}$ and Phe-tRNA$^{Phe}_{h\nu}$ are compared (Tables I and II).

The findings are consistent with identical elementary steps for both native and cross-linked Phe-tRNA. If this were all, the steady-state kinetics of AMP-dependent deacylation of Phe-tRNA$^{Phe}_{h\nu}$ could be understood on the basis of the proposal (Holler, 1976) and the conformer distribution (eq 17). The Michaelis–Menten constant would reflect binding of Phe-tRNA$^{Phe}_{h\nu}$ to the tRNA-specific site of the enzyme since this mode of complex, although nonproductive, competes with the

association to the Phe-specific site. The value of the catalytic rate constant would be the first-order rate constant, k_f(1st), that is calculated from the association rate constant, k_f, for binding to the Phe-specific site. The values would be K_m = 0.35 μM and k_{cat} = 0.46 s^{-1}. The corresponding equilibrium constant of the overall reaction, K_{eq}', is then calculated to be 0.4 (eq 10). The value would be in excellent agreement with K_{eq}' = 0.6 calculated for native tRNA (see above). However, the experimental values are k_{cat} = 0.01 s^{-1} and K_{eq}' = 19. The value K_m = 0.33 μM is compatible with the theoretical value.

This discrepancy can be accounted for by assuming that only the conformer T_1 (eq 17) undergoes AMP-dependent deacylation:

$$E + T_1 \xrightarrow{k_{cat}(true)} E + \text{products} \quad (18)$$

$$\frac{d[\text{products}]}{dt} = k_{cat}(\text{true})[E][T_1] \quad (19)$$

All the remainder of reactants have been included in symbol E. We assume in eq 18 that the conformational change during association of Phe-$tRNA_{h\nu}^{Phe}$ and enzyme at the Phe-specific binding site is rate limiting (Holler, 1976, 1980) and that k_{cat}(true) resembles the apparent first-order rate constant k_f(st). It would be observed as $k_f K_{diss}^{(1)}$ (eq 3) when T_1 reacts according to eq 1 and 2. A combination of the conservation equation

$$[T]_0 = [T_1] + [T_2] + [T_1'] + [T_2'] \quad (20)$$

with the definition of conformer equilibrium constants (eq 17) leads to the expressions

$$\frac{d[\text{products}]}{dt} = k_{cat}(\text{app})[E][T]_0 \quad (21)$$

$$k_{cat}(\text{app}) = k_{cat}(\text{true})\left[\frac{K_c}{1 + K_c}\right]\left[\frac{K_{c'}}{1 + K_{c'}}\right] \quad (22)$$

For comparison of native and cross-linked Phe-tRNA, we set k_{cat}(true) = 9 s^{-1} (AMP-dependent deacylation of Phe-$tRNA^{Phe}$, Table I). In place of $K_c/(1 + K_c)$, the correction factor $K_{diss}(tRNA^{Phe})/K_{diss}(tRNA_{h\nu}^{Phe})$ = $^1/_{25}$ (Table I) and, in place of $K_{c'}/(1 + K_{c'})$, the correction factor K_{diss}(Phe-$tRNA_{h\nu}^{Phe}$, tRNA site)/$K_{diss}(tRNA_{h\nu}^{Phe})$ = $^1/_{14}$ are chosen. From these values, we calculate k_{cat}(app) for AMP-dependent deacylation of Phe-$tRNA_{h\nu}^{Phe}$ to be 0.02 s^{-1}, in excellent agreement with the experimental value 0.01 s^{-1} (Table I).

In summary, the experimental data for native and cross-linked tRNA are understood on the basis of the following unifying model. (1) $tRNA^{Phe}$ consists of at least two conformers at equilibrium. (2) Cross-linking shifts the equilibrium in favor of a nonbinding conformer. (3) Phenylalanylation introduces additional conformers T_1' and T_2'. The population T_1, T_1', and T_2' binds to the tRNA-specific site of the enzyme. (4) Conformers T_1 and T_1' associate with the enzyme at the Phe-specific site. (5) T_1 undergoes enzymatic AMP-dependent deacylation. (6) The reaction paths are identical for both native and cross-linked tRNA and involve the dissociation–association of the enzyme·Phe-tRNA complex at the Phe-specific site as rate-limiting steps.

AMP-Independent Deacylation. AMP-independent deacylation (hydrolysis) of Phe-$tRNA_{h\nu}^{Phe}$ occurs at the tRNA-specific binding site of the enzyme, as is concluded by the similarity of K_m and $K_{diss}^{(1)}$ values (Tables I and II), by the absence of effects of added Phe, and in analogy to hydrolysis of Phe-$tRNA^{Phe}$ (Güntner & Holler, 1979). In contrast to AMP-dependent deacylation, most or all of the conformers that bind are also deacylated. This is concluded from the fair agreement of the k_{cat} value 0.013 s^{-1} with the value k_{cat} = 0.018–0.026 s^{-1} for Phe-$tRNA^{Phe}$ in the presence of Phe (Güntner & Holler, 1979).

Conclusion

The features of the reaction of cross-linked $tRNA^{Phe}$ can be deduced from those of native $tRNA^{Phe}$, including existing conformer equilibria. We are aware that conformers are overemphasized by this explanation. Future work is needed to distinguish from genuine enzyme-induced conformational changes. Interactions that are responsible for maintaining conformers have not been characterized. Perhaps the -CCA acceptor end may not be that rigid (Sprinzl & Cramer, 1979) to exclude the formation of conformers if the remainder of the tRNA body offers a possibility of an interaction. Modification of the 3′-terminal adenosine, including cognate and noncognate aminoacylation, may affect conformer distribution. The possibility could shed new light on the concept of "reacting site triggering" of the terminal adenosine (von der Haar & Cramer, 1978) or on the understanding of recognition of noncognate aminoacyl-tRNA during hydrolytic proofreading. One important aspect of conformer equilibria is, as demonstrated by the case of cross-linked $tRNA^{Phe}$, that a single modification of tRNA (phenylalanylation) might have a marginal effect on binding and reaction constants but could become important in the presence of a second modification (cross-linking).

References

Bartmann, P., Hanke, T., & Holler, E. (1975a) *J. Biol. Chem. 250*, 7668–7674.

Bartmann, P., Hanke, T., & Holler, E. (1975b) *Biochemistry 14*, 4777–4786.

Carrê, D. S., Thomas, G., & Favre, A. (1974) *Biochimie 56*, 1089–1101.

Crothers, D. M., & Cole, P. E. (1978) in *Transfer RNA* (Altman, A., Ed.) pp 196–247, MIT Press, Cambridge, MA.

Dietrich, A., Kern, D., Bonnet, J., & Ebel, J.-P. (1976) *Eur. J. Biochem. 70*, 147–158.

Eadie, G. S. (1942) *J. Biol. Chem. 146*, 85–93.

Favre, A., & Yaniv, M. (1971) *FEBS Lett. 17*, 236–240.

Favre, A., Ballini, J. P., & Holler, E. (1979) *Biochemistry 18*, 2887–2895.

Güntner, C., & Holler, E. (1979) *Biochemistry 18*, 2028–2038.

Haldane, J. B. S. (1930) in *Enzymes*, Longmans, Green and Co., New York.

Hanke, T., Bartmann, P., Hennecke, H., Kosakowski, H. M., Jaenicke, R., Holler, E., & Böck, A. (1974) *Eur. J. Biochem. 43*, 601–607.

Holler, E. (1976) *J. Biol. Chem. 251*, 7717–7719.

Holler, E. (1980) *Biochemistry 19*, 1397–1402.

Holler, E., & Kosakowski, H. M. (1973) *Biochem. Biophys. Res. Commun. 54*, 1532–1539.

Holler, E., Schwarze, G., Scheibl, R., & Hammer-Raber, B. (1980) *Biochemistry 19*, 5403–5411.

Kim, S. H., Quigley, G. J., Suddath, F. L., McPherson, A., Sneden, D., Kim, J. J., Weinzierl, J., & Rich, A. (1973) *Science (Washington, D.C.) 179*, 285–288.

Kosakowski, H. M., & Böck, A. (1970) *Eur. J. Biochem. 12*, 67–73.

Kosakowski, H. M., & Holler, E. (1973) *Eur. J. Biochem. 38*, 274–282.

Pimmer, J., & Holler, E. (1979) *Biochemistry 18*, 3714–3723.
Ramabhadran, T. V., & Jagger, J. (1976) *Proc. Natl. Acad. Sci. U.S.A. 73*, 59–69.
Rupley, J. A., & Gates, V. (1967) *Proc. Natl. Acad. Sci. U.S.A. 57*, 496–510.
Santi, D. V., & Anderson, R. T. (1974) *Anal. Biochem. 58*, 175–182.
Sprinzl, M., & Cramer, F. (1979) *Prog. Nucleic Acid Res. Mol. Biol. 22*, 1–69.
Stuhlberg, M. P. (1967) *J. Biol. Chem. 242*, 1060–1064.
Thomas, G., & Favre, A. (1975) *Biochem. Biophys. Res. Commun. 60*, 1454–1461.
Thomas, G., & Favre, A. (1977) *C. R. Hebd. Seances Acad. Sci., Ser. D 284*, 1345–1347.
von der Haar, F., & Cramer, F. (1978) *Biochemistry 17*, 3139–3145.
Yarus, M. (1972) *Proc. Natl. Acad. Sci. U.S.A. 69*, 1915–1919.

Nuclear Magnetic Resonance and Nuclear Overhauser Effect Study of Yeast Phenylalanine Transfer Ribonucleic Acid Imino Protons†

Paul D. Johnston‡ and Alfred G. Redfield*

ABSTRACT: Results directed primarily toward spectral assignment and nuclear spin dynamics are described for yeast $tRNA^{Phe}$ in 0.1 M NaCl, pH 7. Magnesium titrations were performed. Changes in the spectrum occur for Mg^{2+}/tRNA ratios of about 2 and above 10. Difference spectroscopy between 43 and 29 °C in zero Mg^{2+} concentration, together with prior identification of the GU4 acceptor stem base pair, indicates early acceptor melting and is used to identify acceptor resonances. Transport of spin energy (spin diffusion) is described in tRNA together with a summary of relevant experiments. A survey of nuclear Overhauser effects (NOE's) between imino and aromatic and amino protons is included, together with some recent conclusions based on methyl NOE's and experiments with tRNAs deuterated at the purine C8 position. Assignment of the imino NMR spectrum on the basis of these and previous data is reviewed and discussed in detail. Preliminary distance estimates based on the NOE for AU and GU4 base pairs are in reasonable agreement with the expected distances.

The NMR spectrum of transfer ribonucleic acid (tRNA)[1] provides useful indicators of conformation and dynamics because both the extreme upfield methyl region of the spectrum and the extreme downfield imino region are relatively uncluttered and potentially amenable to assignment. The imino protons are especially interesting (Kearns & Shulman, 1974) because the rates of their exchange with solvent can be measured by NMR in order to obtain information on structural mobility (Crothers et al., 1974; Johnston & Redfield, 1977). Despite much work and progress, assignment of the imino resonance region to specific secondary and tertiary protons is not as complete as is desirable for further applications to biologically relevant problems (Reid & Hurd, 1977; Bolton & Kearns, 1978; Kearns & Bolton, 1978; Patel, 1978; Robillard & Reid, 1979; Schimmel & Redfield, 1980).

This article summarizes our work directed primarily toward assigning the imino region of the spectrum of yeast $tRNA^{Phe}$ on the basis of observations of the nuclear Overhauser effect (NOE) and also on the temperature and magnesium dependence of the spectrum, as well as solvent exchange rates. In a subsequent article, we will present work on the dynamics of unfolding of tRNA measured by NMR. Preliminary publications of this work have appeared (Johnston & Redfield, 1977, 1978), including an introductory exposé (Johnston & Redfield, 1979).

In order to orient our later discussion, we first describe the NMR spectrum at low and moderate temperature as a function of magnesium ion concentration and describe transport of proton spin energy ["spin diffusion"; see Kalk & Berendson (1976)] in tRNA. This is relevant to our observations of the nuclear Overhauser effect in tRNAs as well as to studies of thermal unfolding at higher temperatures.

We then turn to the NOE observations, which tell us unequivocally that pairs of proton resonance lines in the spectrum come from pairs of protons which are adjacent to each other in the structure. Combined with information about the tertiary structure, and NMR experience with model compounds, the NOE can yield new assignments and distance information in favorable cases, and also permits clean resolution of many otherwise obscure NMR lines.

The nuclear Overhauser effect has been described in our earlier papers (Redfield & Gupta, 1971; Johnston & Redfield, 1979). Briefly, it consists of application of a long (0.05–0.5 s) weak preirradiation pulse of radio frequency power at a frequency, f_2, designed to wipe out or saturate a single NMR line at that frequency by pumping energy into the protons resonating at f_2 only. This pulse is followed immediately by an observation pulse, which is especially designed to not excite the strong water resonance. The NMR signal produced by

† From the Department of Biochemistry, Brandeis University, Waltham, Massachusetts 02254. *Received July 1, 1980.* This work was supported in part by U.S. Public Health Service Grants GM20168 and 5T01-GM0212 and by the Research Corporation. This is Publication No. 1335 of the Brandeis University Biochemistry Department. A.G.R. is also at the Physics Department and the Rosensteil Basic Medical Sciences Research Center of Brandeis University.

‡ Present address: Institute of Molecular Biology, University of Oregon, Eugene, OR 97403.

[1] Abbreviations used: tRNA, transfer ribonucleic acid; NOE, nuclear Overhauser effect; EDTA, ethylenediaminetetraacetic acid; T, ribothymidine; m^1A, N^1-methyladenosine; m^2G, N^2-methylguanosine; m^2_2G, N^2-dimethylguanosine; m^7G, N^7-methylguanosine; Ψ, pseudouridine; s^4U, 4-thiouridine.

0006-2960/81/0420-1147$01.25/0